RESEARCH PAPER

Low-Cost Fabrication and Surface Engineering of Insulating KBr Crystals: An AFM Study on the Effects of Thermal Annealing

Asieh Sadat Kazemi*, Maryam Hashemi, Mohamad Mohamadnezhad

* *asiehsadat_kazemi@iust.ac.ir*

Surface Physics Lab, Department of Physics, Iran University of Science and Technology

Received: March 2024 **Revised: December 2025** **Accepted: February 2026**
DOI: 10.22068/ijmse.3566

Abstract: *The crystal structure of potassium bromide (KBr) attracts attention due to its various applications in electronic and optical devices and its potential to induce local electrostatic fields. Fabricating this crystal via the conventional Czochralski method or more novel epitaxial methods is very costly. Here, with the focus on surface properties, a simple, low-cost technique is employed using KBr powder, pellet-making, and a pressure appliance to fabricate pellet crystals. These pellets have been annealed at various temperatures and studied by atomic force microscopy for morphological and structural analysis. Our results demonstrate that increasing the temperature before the KBr melting point significantly reduces roughness parameters, including the height and spacing of atomic steps. At 500°C, the atomic steps are more regular than at other temperatures, surface flatness and crystallinity are enhanced, approaching the quality of commercial single crystals. These modifications improve the quality of the crystals significantly, for various applications. Force spectroscopic measurements across atomic step edges of KBr reveal higher forces than in flat regions. These engineered steps could serve as nanoscale templates for directing the self-assembly of molecules or for creating spatially varying electrostatic potentials in 2D material heterostructures.*

Keywords: *KBr crystal, AFM, Atomic steps, Roughness, Force spectroscopy.*

1. INTRODUCTION

KBr has a clear and uniform FCC crystal, it is highly transparent in the mid-infrared (IR) region and non absorbing for most IR wavelenghts, also has high permeability and a wide bandwidth [1], commonly used in IR Fourier transform spectroscopy (FTIR) and beam splitters in spectrophotometers due to its low phonon absorption and in scintillators [2, 3]. KBr is also colorless and due to its ionic nature, is soluble in water, and has a melting point of 734°C. KBr substrates are soft and moist, and have good resistance to mechanical shocks [4]. Since they cleave readily along (100) planes, they are used for thin-film growth [5], for the production of soft electronic components as electrical insulators, and as a support for molecular adsorption studies in UHV systems [6]. Terrace modifications of KBr as an ionic substrate at the atomic level have been used to generate electrostatic potentials on 2D materials [7]. KBr pellets have recently been used to assess the photodimerization (i.e., the photochemical reaction) of acid compounds [8]. Furthermore, KBr is used as a light transducer for ultraviolet and soft X-ray components in the 10-200 nm range [9]. KBr thin films are feasible alternatives for ultraviolet (UV) and soft X-ray photocathode devices due to their high quantum efficiency and good stability in the extreme ultraviolet to vacuum ultraviolet regions [10]. They can also be used as a protective layer in visible-sensitive photon detectors [11]. Owing to the lower photoconversion efficiency of the KBr photocathode in the far ultraviolet (FUV) wavelength region, signal quality may be improved by rejecting sources of radiation and background near-UV wavelengths [12]. The crystal surface of many oxides and alkali halides, such as KBr, differs from their bulk due to dangling bonds and surface irregularities, including dislocations, vacancies, and defects in the periodicity of the crystal. These surface features and broken periodicity at the termination planes can evolve dynamically under environmental influences, such as vapour adsorption, leading to distinct surface energies and structural rearrangements [13, 14], highlighting the importance of dedicated surface studies to understand real material behaviour beyond ideal bulk lattice models. A monocrystalline solid is a material in which the crystal lattice of the entire sample, from the mass to the edges of the piece, is continuous and unbroken. The absence of defects gives single crystals unique mechanical, optical, and electrical properties with respect to polycrystals [15]. Specific methods for producing single crystals include the Czochralski process, the floating-zone process,

[DOI: 10.22068/ijmse.3566]

and the Bridgman method [16, 17], and some, like Czochralski's furnace, cost at least $400,000. The main techniques of KBr crystal growth can be divided into four categories: molten, solid, vapor, and soluble. Other crystallization methods vary depending on the material's physical properties, such as hydrothermal synthesis, sublimation, simple solvent-based crystallization [6] or epitaxy [18]. The laying method is used to place thin layers (micro- or nanometer-thick) of similar or different materials on the surface of a crystal. This method has been influential in producing polar plates (111) of potassium bromide, which is electrostatically unstable under normal conditions [19]. However, vacuum-based assembly methods are very expensive, increasing the cost of crystal production.

Given the importance of surface studies and the critical role of surface quality in the mentioned applications, and given the current high cost of these methods, we report a simple, low-cost approach to achieve high-quality flat KBr surfaces, followed by thorough characterisation to determine the optimal conditions. In the inexpensive method, transparent, pressurised pellets were heated to different temperatures in the furnace and examined under an optical microscope. FTIR explored the water evaporation mechanism at different annealing temperatures in KBr pellets, while the overall crystal structure of the pellets was investigated by X-ray diffraction (XRD). The surface morphology and step edges. The roughness and adhesive force of these crystals were characterised by atomic force microscopy (AFM) in contact mode and compared with a standard KBr substrate in terms of surface flatness, the number and spacing of atomic steps, and the adhesive force at various annealing temperatures.

2. EXPERIMENTAL PROCEDURES

Spectroscopic-grade quality KBr powder (Merck) with a particle size of 100–200 mesh (~100 μm) [18] was first ground in a unique, pre-cleaned opal mortar to give a uniform texture. The softened powder was evenly placed inside the 1 cm-diameter pellet holder. The holder containing the uniform powder was placed in a press unit, and the pellets were fabricated using a laboratory hydraulic pellet press with a maximum capacity of 15 tons. The powder was pressed in a 1 cm-diameter die, applying approximately 8 tons of force. Using a similar method, several pellets were fabricated for reproducibility and for annealing at various temperatures. Next, the pellets were placed in clean ceramic boats and into the furnace. The furnace was heated in 50°C increments to reach the desired temperatures of 350°C, 400°C, 450°C, 500°C, 550°C, and 600°C, and held for an hour. The furnace temperature was then reduced stepwise to room temperature (RT) to prevent heat shock in the pellets. All samples were kept in a vacuum desiccator. For the comparison study, a KBr (100) crystal was purchased from Agar Scientific (trade ID AGG3900) and cleaved at a right angle with a sharp blade. FTIR spectroscopy (Perkin Elmer 100) was performed on all pellets before the annealing process. Crystallography was achieved on the samples with an X-ray diffractometer (XRD) system (Bruker-Advanced), and further analyses on the crystal planes and orientations were conducted with XPert software. FTIR and XRD results and discussions are presented in the Supporting Information (SI). Topography imaging and force spectroscopy were performed with an atomic force microscope (Advanced-Ara Pajuhesh) at RT, with a humidity of 30%, where the KBr surface remained protected. Contact mode with low force was used with HQ: CSC17/AlBS cantilever purchased from MikroMasch, with a force constant of 0.18 N/m and a resonance frequency of 13 kHz. The material of the cantilever was n-type Si. These AFM cantilevers with low force constants offer high sensitivity in contact mode, high consistency of tip radius, cantilever reflectivity and the quality factor. The set point was kept at 0.65 of the reference voltage, and the can rate was 1 line/s.

3. RESULTS AND DISCUSSION

3.1. Atomic Steps

The formation of atomic steps of KBr at 350°C, 400°C, 450°C, 500°C, 550°C, and 600°C was investigated using AFM. These surface measurements of the KBr revealed terraces with widths ranging from 1.40 μm to 6 μm. Figure 1 shows 2D and 3D AFM images of KBr surfaces in contact mode. On the surface of KBr at 350°C, there appear to be no specific atomic steps in the imaging window, but they may be much farther away. It is evident that the distance between atomic steps decreases with increasing temperature; thus, the atomic steps become closer. In addition, the height of the steps decreases with increasing temperature. Borderline-like lines on the image surfaces may be due to

[DOI: 10.22068/ijmse.3566]

stresses generated during the pellet-making process and are visible in all images, regardless of the annealing temperature. At 500°C, the atomic steps are more regular and sharper than at other temperatures. As the temperature increases to 550°C and 600°C, the atomic steps begin to merge, lose regularity, and become rounded, transitioning towards lower-energy steps. As the pellets approached their melting point, their crystal structure deteriorated, consistent with the evolution of the XRD spectra in the SI, where the peak intensities were highest at 450°C and 500°C. Figure 2 (b) shows the variation of the distance between the atomic steps in annealed KBr pellets with temperature. With increasing temperature, the distance between atomic steps decreased. These data were extracted from images using SPIP software. The observed rounding and straightening of the step edges during annealing indicate a transition from higher-energy, high-Miller-index facets to lower-energy, low-Miller-index facets, consistent with thermodynamically favoured surface restructuring [20, 21].

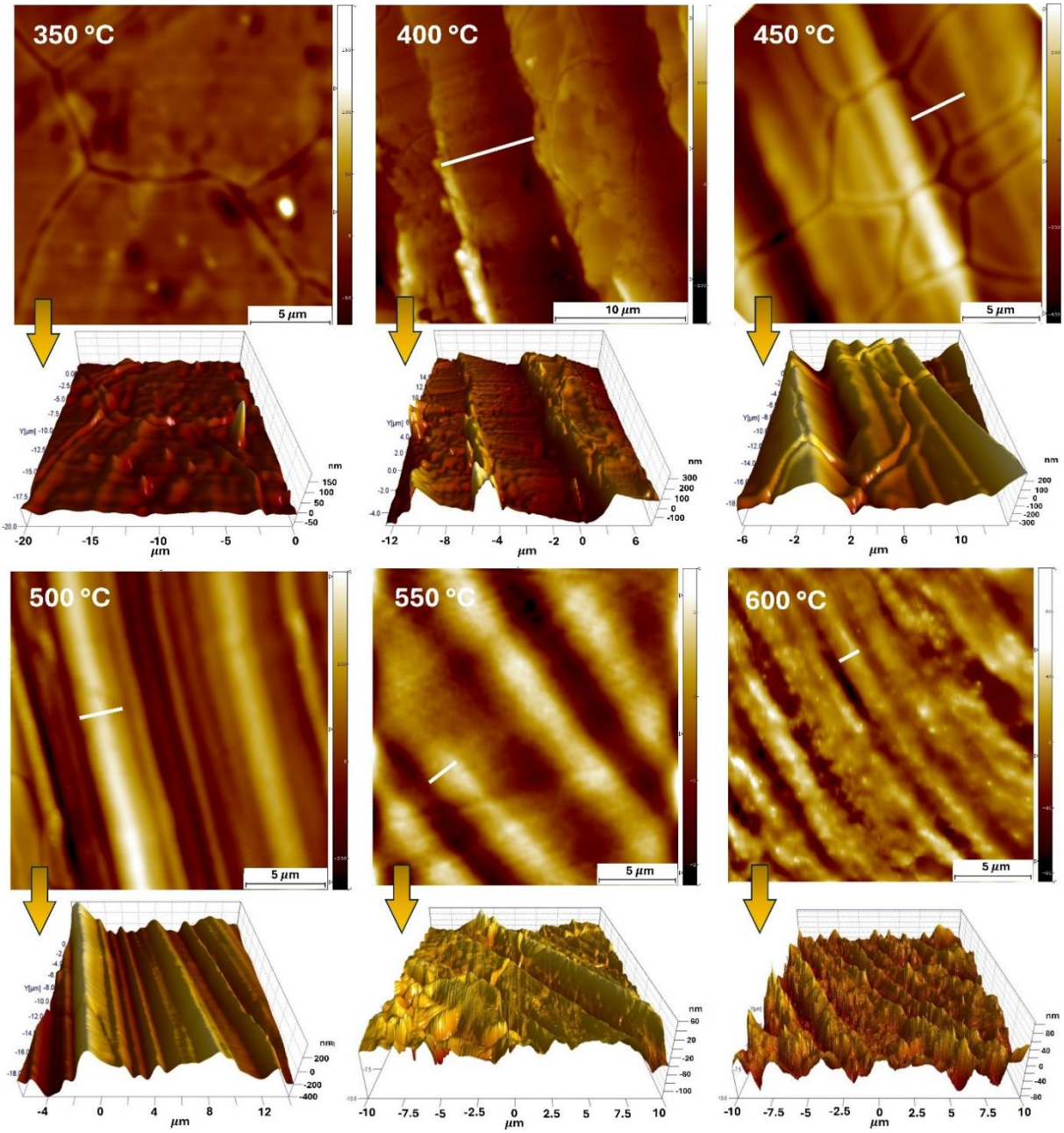

Fig. 1. 2D and the corresponding 3D AFM topographic images of the surface of KBr pellets in contact mode at different annealing temperatures; all with dimensions of 20μm×20 μm

[DOI: 10.22068/ijmse.3566]

Figure 2(c) schematically shows the evolution of high-index steps into low-index steps with increasing annealing temperature at a cubic crystal step edge. Although atomic-sized transitions beyond 500°C require high-resolution microscopy, such as a tuning fork non-contact AFM, evidence of step boundary features can be seen on the surface of the 500°C sample in Figure 2(a), where a boat-shaped feature is enlarged. This shape can constitute many high-index steps if atomically resolved. 2D and 3D AFM images of the as-purchased crystalline KBr, used as a reference for this study, in Figures 2(d,e), show ultra-regular atomic steps with very short spacing. The steps in KBr pellets at 500°C are closest to this sample.

3.2. Roughness Variation with Annealing Temperature

Accurate surface roughness studies of KBr at different annealing temperatures require equally sized imaging windows free of atomic steps or stress boundaries. Therefore, 2 µm ×2 µm windows were isolated from 2D images in Figure 1 in a region between a pair of atomic steps depicted in Figure 3(a). The roughness parameters of these images were processed in SPIP and summarised in Figure 3(b). Roughness parameters of the reference sample were also extracted for comparison. Sa, being the most common roughness parameter reported in the literature, is the average roughness, or the average of the deviations from the mean plane, and varies with annealing temperature, as shown in Figure 3(c). Sq is the RMS roughness, which is also commonly used, and is the standard deviation of the height distribution. Sz is the difference between Sp and Sv, while Sp shows the maximum peak height and Sv shows the maximum valley depth.

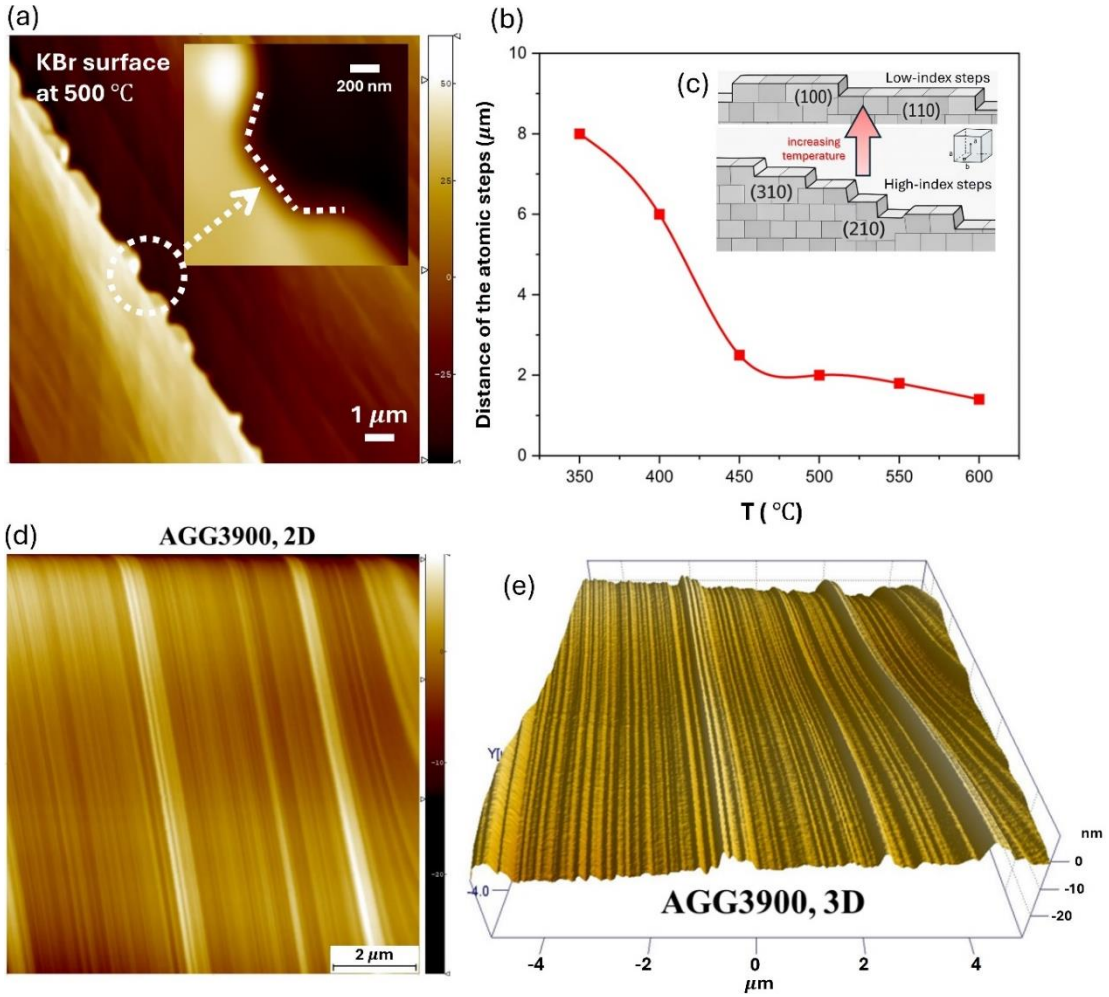

Fig. 2. a) 2D AFM image of a step edge with boat shape boundary, b) The average distances of the atomic steps in annealed KBr samples at different temperatures, c) Schematics of step transitions with the increase in temperature, d,e) 2D and 3D images of AGAR Scientific KBr crystal with trade ID AGG3900

[DOI: 10.22068/ijmse.3566]

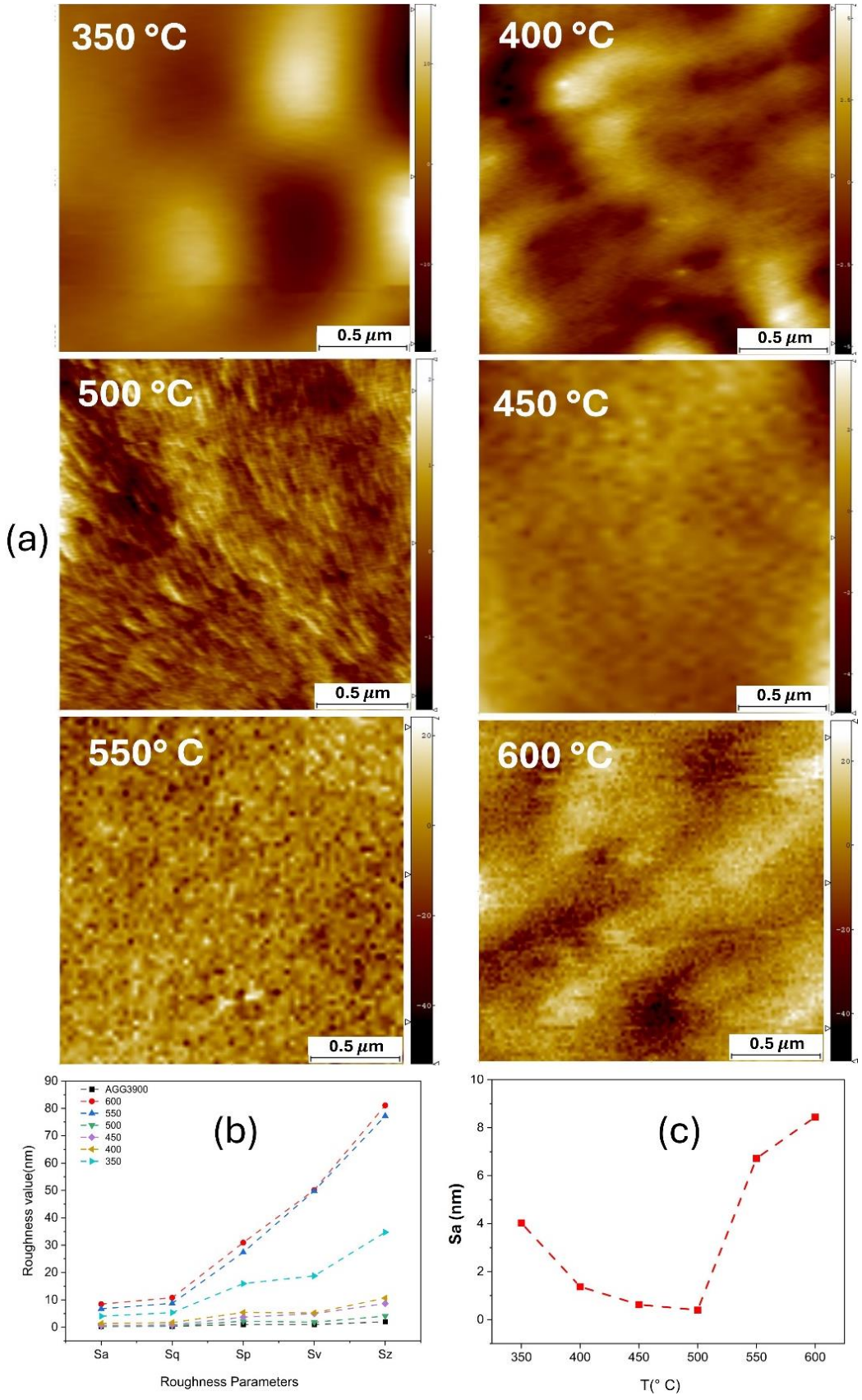

Fig. 3. a) 2D topographic images of the surface of KBr pellets at different annealing temperatures, b) Variation of roughness parameters extracted from the 2D images in part a,c) Sa variation with annealing temperature

[DOI: 10.22068/ijmse.3566]

The surface roughness, Sa, decreased markedly with increasing annealing temperature up to 500°C. Beyond that, Sa increased rapidly to values higher than 5 nm. Again, from previous analyses, it is known that beyond this point, the surface crystallinity deteriorates. Another quantity extracted from the surface roughness, Sq, has a similar variation to Sa. The other two standard parameters, Sp and Sv, indicated small variations (below 10 nm) in the reference KBr and in those annealed at 400°C, 450°C, and 500°C. However, at 350°C, 550°C, and 600°C, these parameters increase to much higher values, up to 50 nm. Sz, being calculated from Sp and Sv, showed a similar trend. This means the highest peak height and deepest valley depth in less crystalline samples are higher, and this agrees with XRD results. In short, the initial reduction in surface roughness up to 500°C can be attributed to enhanced surface diffusion and increased atomic mobility, which promote the relaxation of surface irregularities and step edges, and the elimination of defects, in agreement with [22]. At higher temperatures, however, all roughness values increased rapidly, likely due to surface instability, defect formation, and partial degradation of surface crystallinity as the material approached thermally activated disordering or pre-melting phenomena as commonly observed for alkali halide surfaces such as KBr.

3.3. Force Spectroscopy across Atomic Steps

According to the AFM roughness and XRD results, annealed KBr samples around 500°C demonstrated a higher degree of crystallinity. Some of the samples were selected for force spectroscopy. This process was performed point by point on the surface by switching off the feedback loop and applying a specific indentation to the substrate, enabling detection of the pull-off force (the maximum attractive force during tip retraction in each force–distance curve). Figure 4 shows 2D images of atomic steps on KBr pellets annealed at 450°C, 500°C, and 550°C, and on the reference purchased KBr. Force spectroscopy was performed with only a few nanometers of indentation, well within the elastic deformation regime and non-destructive for the KBr crystal. The force variation across these steps, measured in nN, showed higher forces at the step boundaries, while flatter regions had lower adhesive forces. The increased adhesion observed at the step edges can be attributed to the higher local surface energy at these sites. Step edges and defect sites are more likely to adsorb ambient water molecules, which enhances capillary forces. In addition, the intrinsic ionic polarization at the step may increase local electrostatic interactions between the tip and surface, further contributing to the elevated adhesive force [23]. This property of atomic steps can be exploited for electrostatic potential tuning on bare KBr or KBr covered with 2D materials, where screening effects remain minor, as predicted theoretically and demonstrated by electric force microscopy and scanning tunnelling microscopy/spectroscopy [24, 25].

3.4. FTIR and XRD Analyses

The evolution of water with annealing temperature in KBr pellets was examined via FTIR spectroscopy in SI and Figure S1. The results agreed with [2, 26, 27]. XRD data were collected from pellets using monochromated CuKα (λ=1.54060 Å) radiation with 2θ from 5° to 85°. XRD spectra of the annealed pellets are depicted in Figure S2, confirming an FCC crystal structure and agreeing with the literature [28]. XRD patterns of KBr pellets exhibit the most intense peak at the (200) crystallographic plane; this peak is from the peak family of (100) and is essential in potassium bromide crystals, followed by other peaks at (111), (220), and (420) planes, respectively. For better clarity, the significant peaks are zoomed in on in Figure 1. The zoomed-in images of the (111) peak at 350°C and 400°C show low intensity. At 450°C and 500°C, the peak intensity increases. With further increase in annealing temperature to 550°C and 600°C, the intensity of this peak decreases to its lowest value in agreement with [29, 30].

4. CONCLUSIONS

Inexpensive and simple methods were used to produce KBr crystal structures and to tune crystal properties via a pressurised powder and annealing process. KBr has many applications across different fields, and the easier fabrication of this material with tuned crystallinity is desired. Structural and morphological study, along with intensive AFM imaging, roughness measurements, and force spectroscopy, was performed on KBr samples annealed at 350°C to 600°C, just below its melting temperature, and on a reference KBr substrate for comparison. The results demonstrated that the optimal annealing temperature was 500°C, where higher crystallinity on the surface, the best agreement with the reference sample, reduced average roughness (Sa) to 0.4 nm, and reduced step spacing to 2 μm.

[DOI: 10.22068/ijmse.3566]

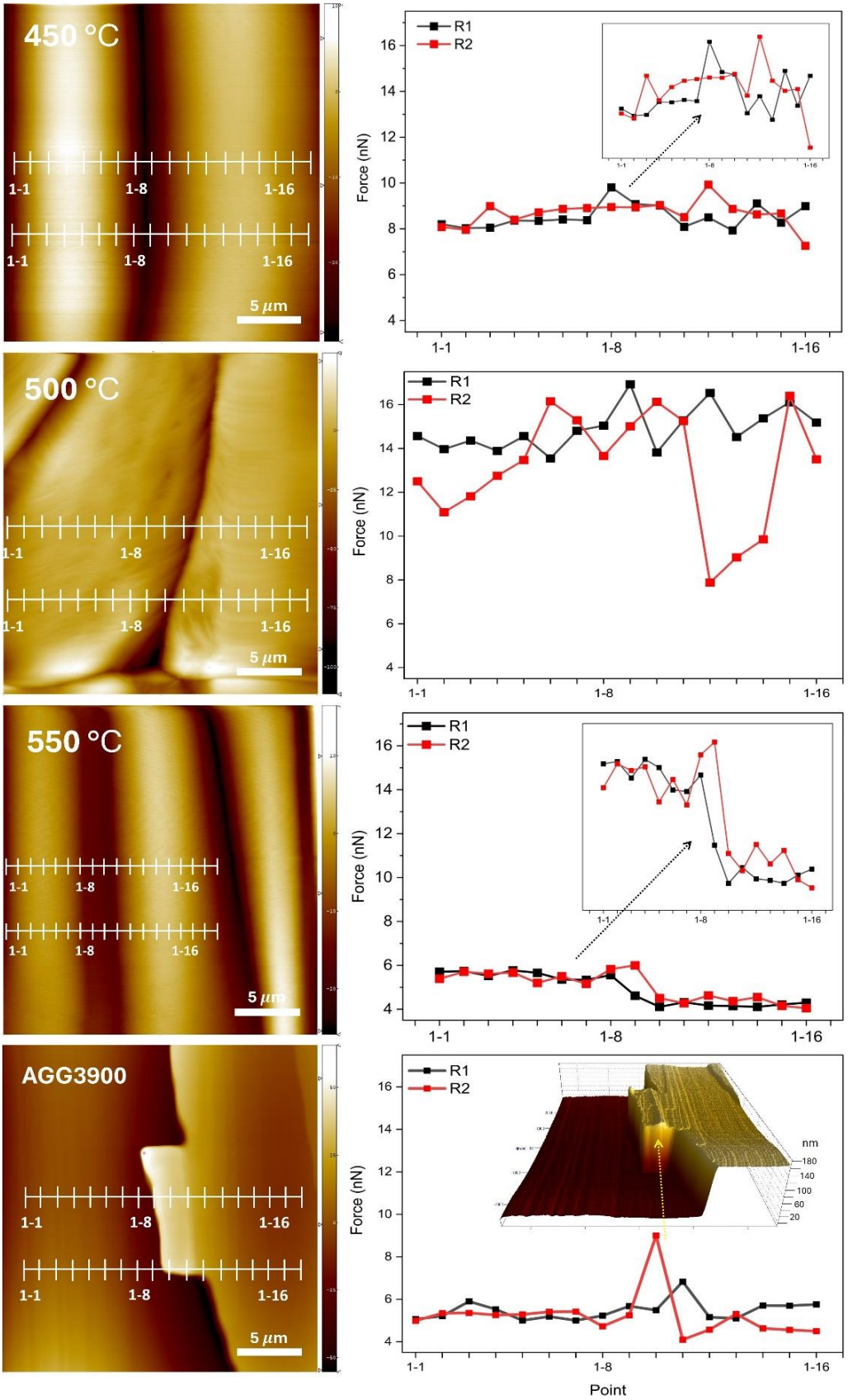

Fig. 4. 2D AFM topographic images of KBr samples at 450°C, 500°C, 550°C and the reference KBr sample, along with pull-off force variations across relevant atomic steps

[DOI: 10.22068/ijmse.3566]

Force spectroscopy measurements showed a larger adhesive force on atomic steps than on flat regions. We propose that these engineered steps could serve as nanoscale templates for directing the self-assembly of molecules or for creating spatially varying electrostatic potentials in 2D material heterostructures, which could be probed by Kelvin Probe Force Microscopy (KPFM).

REFERENCES

[1] Singh, S. P., et al., Optical and luminescence properties of alkali halide crystals, Journal of Luminescence, 2008, 128, 1379–1384.

[2] Chalmers, J., Infrared spectroscopy, Encyclopedia of Analytical Science (Second Edition), Elsevier, 2005, 402-415.

[3] Lin, L. Y. et al., Study of scintillation stability in KBr, YAG: Ce, CaF2:Eu and CsI:Tl irradiated by various-energy protons, International Beam Instrumentation Conference, 2014, IBIC.

[4] Villars, P., KBr Crystal Structure, Pauling File Multinaries Edition in: Inorganic Solid Phases, Springer Materials, Springer, 2023, Heidelberg (ed.) SpringerMaterials.

[5] Xu, T., Cai, Q., Duan, W., Wang, K., Jia, B., Luo, H., & Liu, D., Effect of Substrate Temperature on the Structural, Morphological, and Infrared Optical Properties of KBr Thin Films. Materials, 2025, 18(15), 3644.

[6] Glatzel, T., Zimmerli, L., Kawai, S., Meyer, E., Fendt, L. A. & Diederich, F., Oriented growth of porphyrin-based molecular wires on ionic crystals analyzed by NC-AFM, Beilstein J. Nanotechnol., 2011, 2, 34–39.

[7] Jones, G. J., Kazemi, A., Crampin, S., Phillips, M., Ilie, A., Surface Potential Variations in Graphene Induced by Nanostructured Crystalline Ionic Substrates, Applied Physics Express, 2012, 5 (4), 045103.

[8] Ulambayar, B., Batchuluun, K., Bariashir, C., Uranbileg, N., Stammler, F. J., Davaasambuu, J., & Schrader, T. E., Using potassium bromide pellets and optical spectroscopy to assess the photodimerization of two trans-(trifluoromethyl)-cinnamic acid compounds. CrystEngComm, 2024, 26, 4470–4477.

[9] Rai, R., Triloki, Singh, B. K., Photoemission and morphological studies of KBr thin-film photocathode for astrophysics application, Proceedings of the DAE-BRNS Symp. On Nucl. Phys. 2016, 61.

[10] Oswald H.W. Siegmund, E. Everman, J.V. Vallerga et al., Ultraviolet quantum detection efficiency of potassium bromide as an opaque photocathode applied to microchannel plates, Appl. Opt. 1987, 26, 3607.

[11] Breskin, A., Buzulutskov, A., Chechik, R. et al., Evidence for thin film protection of visible photocathodes, Appl. Phys. Lett., 1996, 69, 1008.

[12] Oswald H.W. Siegmund, D.E. Everman, J.V. Vallerga et al., Soft x-ray and extreme ultraviolet quantum detection efficiency of potassium bromide photocathode layers on microchannel plates, Appl. Opt., 1988, 27, 1568.

[13] Alherz, A., & Alayyoub, B. A., Evaluation of Surface and Bulk Properties of Alkali Halides: A First-Principles Study on (100) and (110) Facets, ACS Omega, 2025, 10(44), 52794–52803.

[14] Pokorny, P., Novotny, M., Dekhtyar, Y., Lushchik, A., Hruska, P., Fara, J., Fitl, P., Musil, J., Jaaniso, R., Lancok, J., Surface processes on KBr single crystals examined by thermostimulated exo-electron emission and desorption, Optical Materials, 2021, 114, 110898.

[15] Milisavljevic, I., Wu, Y., Current status of solid-state single crystal growth, BMC Mat, 2020, 2, 2.

[16] Müller, G., Friedrich, J., Crystal growth, bulk: methods. In: Bassani G, Liedl G, Wyder P, editors. Encyclopedia of condensed matter physics. Oxford: Elsevier Ltd; 2005, 262–74.

[17] Suan Jen Hsueh Pao, K., Growth Process of Large Section Crystal of Potassium Bromide, Journal of the Chinese Ceramic Society, 2015, 43(1), 60-64.

[18] Kato, S., Takeyama, Y., Maruyama, S., and Matsumoto, Y., Nonfaceted Growth of (111)-Oriented Epitaxial Alkali-Halide Crystals via an Ionic Liquid Flux in a Vacuum, Crystal Growth & Design, 2010, 10(8).

[19] Yamauchi, M., Maruyama, S., Ohashi, N., Toyabe, K. and Matsumoto, Y., Epitaxial growth of atomically flat KBr(111) films via a thin ionic liquid in a vacuum, Cryst. Eng. Comm, 2016, 18, 3399.

[20] Bonzel, H. P., Equilibrium crystal shapes and surface faceting, Progress in Surface

[DOI: 10.22068/ijmse.3566]

Science, 2003, 67(1–3), 45–70.
[21] Erb, D. J., Perlich, J., Roth, S. V. Ralf, Schlage, K., Real-Time Observation of Temperature-Induced Surface Nanofaceting in M-Plane α-Al_2O_3, ACS Appl. Mater. Interfaces, 2022, 14, 27, 31373–31384.
[22] Parida, S., Lacasa, J. S., & Eren, B. Water vapor and alcohol vapor induced healing of the nanostructured KBr surface, The Journal of Physical Chemistry C, 2022, 126(31), 13433–13440.
[23] Snyder, R. G., & Scoles, G. Surface and step-edge effects on adhesion forces measured by AFM, Langmuir, 1991, 7, 2321–2327.
[24] Wu, Y., Computational Studies of Graphene on Nanostructured Ionic Substrates, PhD. Thesis, University of Bath, 2016.
[25] Kazemi, A. S., Engineering the wavefunction in graphene systems, PhD. Thesis, University of Bath, 2015.
[26] Khajelakzay, M., Shoja Razavi, R., Barekat, M., Synthesis and Characterization of Yttria Nanopowders by Precipitation Method, Transactions of the Indian Ceramic Society, 2015, 74(4), 208-212.
[27] Gordon, S. H., Mohamed, A., Harry-O'Kuru, R. E., Imam, S. H., A Chemometric Method for Correcting Fourier Transform Infrared Spectra of Biomaterials for Interference from Water in KBr Discs. Applied Spectroscopy, 2010, 64(4), 448-457.
[28] R. Rai, T. Triloki, B.K. Singh, X-ray diffraction line profile analysis of KBr thin films, Appl. Phys. A, 2016, 122, 774.
[29] Liu, Y., Song, H., Zhang, Q., and Chen, D., A Preliminary Study of the Preparation of a KBr-Doped ZnO Nanoparticle and Its Photocatalytic Performance on the Removal of Oil from Oily Sewage, Ind. Eng. Chem. Res., 2012, 51 (13), 4779–4782.
[30] Unga´r, T., Balogh, L., Riba´rik, G., Defect related physical profile based X ray and neutron line profile analysis, Metall. Mater. Trans. A, 2010, 41, 1202.

[DOI: 10.22068/ijmse.3566]